Zitierweise: *Angew. Chem. Int. Ed.* **2024**, e202405666
doi.org/10.1002/anie.202405666

Spin Frustration | Hot Paper

Stellated cuboctahedron of Fe^{III}

Lucinda R. B. Wilson, Angelos B. Canaj, Daniel J. Cutler, Laura J. McCormick McPherson, Simon J. Coles, Hiroyuki Nojiri, Marco Evangelisti,* Jürgen Schnack,* Scott J. Dalgarno,* and Euan K. Brechin**

Abstract: The solvothermal reaction of $FeCl_2 \cdot 4H_2O$ and $H_4TBC[4]$ in a basic dmf/EtOH solution affords an $[Fe^{III}_{18}]$ Keplerate conforming to a stellated cuboctahedron. Magnetic and heat capacity measurements reveal spin frustration effects arising from the high symmetry. A crossover between inverse and direct magnetocaloric effects is observed at ~10 K for applied-field changes lower than 3 T.

The first use of the term spin frustration can be traced back to Anderson, Toulouse and Kirkpatrick when discussing exchange interactions in spin glasses[1,2] and has subsequently been employed to describe the magnetic behaviour observed in specific 2–3D lattices, such as those of the kagome and pyrochlore structures.[3] The advent of novel 0D structures containing paramagnetic 3d metal ions saw the definition of geometric spin frustration in molecular systems evolve from initial descriptions requiring a degenerate ground state,[4] which was overly prohibitive, to the presence of competing antiferromagnetic exchange interactions,[5] which was overly permissive. More modern interpretations invoke scenarios which, in essence, describe the opposite of bipartiteness[6] and/or systems where the magnetic behaviour cannot be represented by classical spins.[7] Regardless of ones preferred rubric, the effects of spin frustration on the energy spectrum and magnetic properties of molecular coordination compounds are fascinating and include enhanced ground-state degeneracy, low-lying singlet states, non-collinear ground states, unusual magnetisation plateaus and jumps, and attractive magnetocaloric properties.[6] This makes them both academically interesting and potentially useful for applications in, for example, cryogenic refrigeration.[8]

From a synthetic perspective designing spin frustrated molecules is not trivial. One option is to construct odd-numbered wheels[9] such as $[Cr^{III}_8Ni^{II}]$[10] and $[Cr^{III}_9]$.[11] The former is best described as a magnetic Möbius strip that contains an even number of electrons and has a singly degenerate spin ground state, while the latter has either a $S=1/2$ or $S=3/2$ ground state depending on the exact structure type. A second option is to construct high symmetry polyhedra (e.g. Archimedean, Platonic solids / Keplerates) which possess odd numbered faces, i.e. triangles, pentagons, heptagons, *etc.* While the latter are known in polyoxometalate chemistry, the $[Mo_{72}Fe_{30}]$ icosidodecahedron being a pertinent example,[12] they are far less common in complexes containing only 3d metals. Examples are also often restricted to relatively small molecules such as triangles, which are perhaps not as interesting or as potentially useful as larger species since they have a rather simple energy spectrum consisting of one band of energy levels.[13]

In an attempt to construct large, high symmetry cages that may display spin frustration effects we have turned to the use of *p*-tert-butylcalix[4]arene ($H_4TBC[4]$),[14] a ligand possessing a tetraphenolic lower-rim which is predisposed for metal ion binding[15] and which in its maximal μ_5-bridging mode presents a square-pyramidal $[M_5]$ building block (M = metal; Figure 1). We speculated that the self-assembly of this moiety, via additional, 'internal' oxide/hydroxide bridging, should lead to the formation of stellated polyhedra. In

[*] L. R. B. Wilson, Dr. A. B. Canaj, Prof. E. K. Brechin
EaStCHEM School of Chemistry, The University of Edinburgh
David Brewster Road, Edinburgh, EH9 3FJ, Scotland, UK
E-mail: E.Brechin@ed.ac.uk

Dr. D. J. Cutler, Prof. H. Nojiri
Institute for Materials Research, Tohoku University, Sendai 980-8577, Japan
E-mail: nojiri@imr.tohoku.ac.jp

Dr. L. J. McCormick McPherson, Prof. S. J. Coles
EPSRC National Crystallography Service, School of Chemistry
University of Southampton, Highfield, Southampton, SO17 1BJ, England, UK

Dr. M. Evangelisti
Instituto de Nanociencia y Materiales de Aragón (INMA)
CSIC & Universidad de Zaragoza, 50009 Zaragoza, Spain
E-mail: evange@unizar.es

Prof. J. Schnack
Fakultät für Physik, Universitat Bielefeld, Postfach 100131, D-33501 Bielefeld, Germany
E-mail: jschnack@uni-bielefeld.de

Prof. S. J. Dalgarno
Institute of Chemical Sciences, Heriot-Watt University
Riccarton, Edinburgh, EH14 4AS, Scotland, UK
E-mail: S.J.Dalgarno@hw.ac.uk

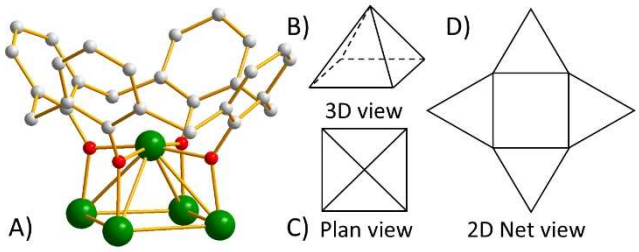

Figure 1. A) The [M_5] square pyramidal building block constructed from TBC[4] in its maximal μ_5-coordination. Colour code: M (metal) = green, O = red, C = grey. ^{t}Bu and H-atoms omitted for clarity. B–D) Representations of Figure A) in 3D, Plan view and 2D Net view, respectively.

order to ensure the maximal bridging mode and the formation of high symmetry species we employ high temperature, high pressure (solvothermal) reactions.

The solvothermal reaction between $FeCl_2 \cdot 4H_2O$ and H_4TBC[4] in a basic dmf/EtOH solution (see the Supporting Information for full details) leads to the formation of black crystals upon slow evaporation of the cooled mother liquor. Crystals of $[Fe^{III}_{18}(\mu_5\text{-}O)_6(\mu_3\text{-}O)_8(\mu_2\text{-}OH)_8(\mu_5\text{-}TBC[4])_4(dmf)_4(H_2O)_2]Cl_2$ were in a cubic cell and structure solution was performed in the *Fm-3c* space group (Table S1, Figure S1). The asymmetric unit (ASU) contains one eighth of the formula and symmetry expansion affords the structure shown in Figures 2–3 (Figure S2, Tables S2–S3). The metallic skeleton describes a stellated cuboctahedron, i.e. a cuboctahedron (Fe2-3 and symmetry equivalents (s.e.)) in which each of the square faces is capped (Fe1, Fe4 and s.e.), the caps themselves forming an octahedron. The six μ_5-O^{2-} ions (O10, O20 and s.e.) connect the four Fe ions in the square faces of the cuboctahedron (Fe2-3 and s.e.) and further bridge to an Fe ion in the octahedron (Fe1). The eight μ_3-O^{2-} ions (O30 and s.e.) bond between the three Fe ions (Fe2, Fe3 and s.e.) in the triangular faces of the cuboctahedron. The eight μ_2-OH^- ions (O1H and s.e.) bridge between an Fe ion in the octahedron (Fe4 and s.e.) and an Fe ion in the cuboctahedron (Fe3 and s.e.). The sixth coordination site on Fe4 (and s.e.) is occupied by a H_2O molecule. The four, fully deprotonated, μ_5-TBC[4] ligands (O1-3 and s.e.) chelate to Fe1 (and s.e.) and further bridge to the square faces of the cuboctahedron (Fe2-3 and s.e.). The sixth coordination site on Fe1 (and s.e.) is occupied by a dmf molecule. Cis and trans Fe–O–Fe bond angles fall in the range 89.18(13)–104.7(5)° and 166.3(11)–170.7(9)°, respectively. Charge balance is maintained through the presence of two Cl^- counter anions.

Examination of the extended structure reveals that six s.e. clusters pack such that they are at the vertices of an octahedron (Figure 4), forming a capsule-like arrangement. This provides a closed shell environment and expansion around a triangular face of this octahedron reveals six clusters arranged in a hexagon. Subsequent expansion around the latter affords an octahedron, and in doing so generates a cuboctahedral assembly (Figures S3–S5). Each cuboctahedron presents a second closed shell environment and, together, these environments constitute ~31 %

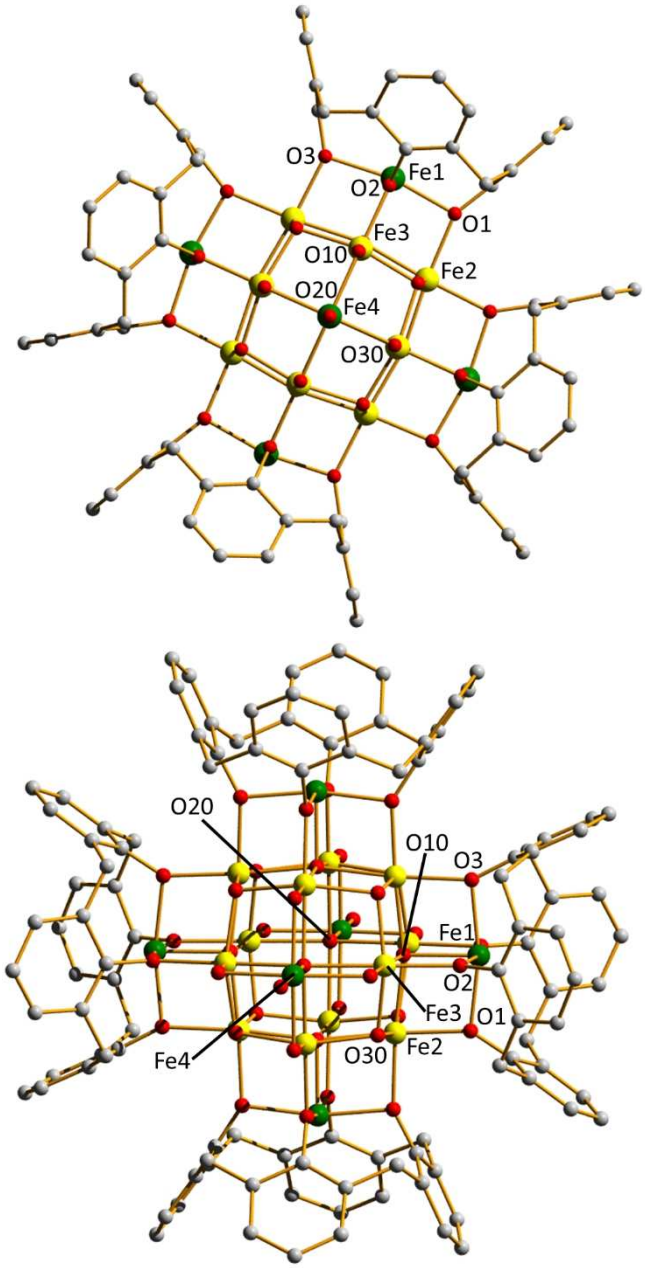

Figure 2. Different views of the molecular cation of complex **1**. Colour code: Fe(octahedron) = green, Fe(cuboctahedron) = yellow, O = red, C = grey. The dmf molecules, ^{t}Bu groups and H-atoms have been omitted for clarity.

(48,027 Å^3) of the unit cell volume (155,525 Å^3) if one employs a 1.5 Å probe radius in contact surface calculations. Inspection of the extended structure reveals that the closest intermolecular Fe···Fe distance is ~12.6 Å—the large TBC[4] ligands provide an encapsulating organic shell around the Fe-oxide core, inducing inherent structural/magnetic dilution in the solid state.

Perhaps surprisingly, compound **1** is the first structurally characterized homometallic cluster of Fe^{III} built using H_4TBC[4], the only previous examples being heterometallic —[Fe_5Gd_4], [Fe_2M_4] (M = Na, K), and [Fe_2Ln_2] (Ln = Gd,

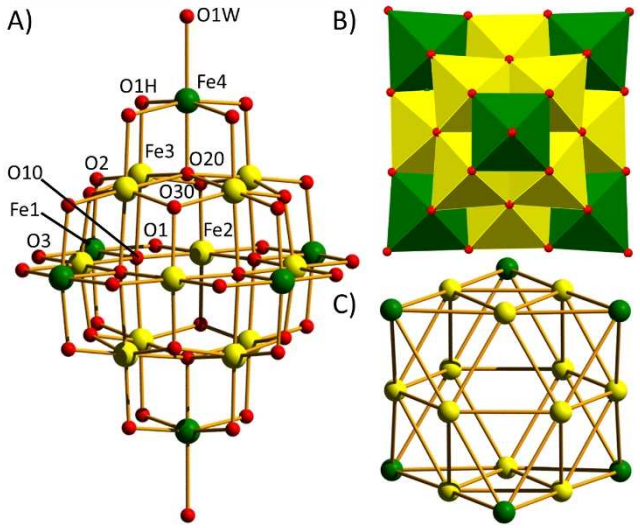

Figure 3. Metal-oxygen core of compound **1** in ball and stick (A) and polyhedral (B) representation. C) Metallic skeleton of **1**. Colour code: Fe(octahedron) = green, Fe(cuboctahedron) = yellow, O = red, C = grey. The dmf molecules, ^{t}Bu groups and H-atoms have been omitted for clarity.

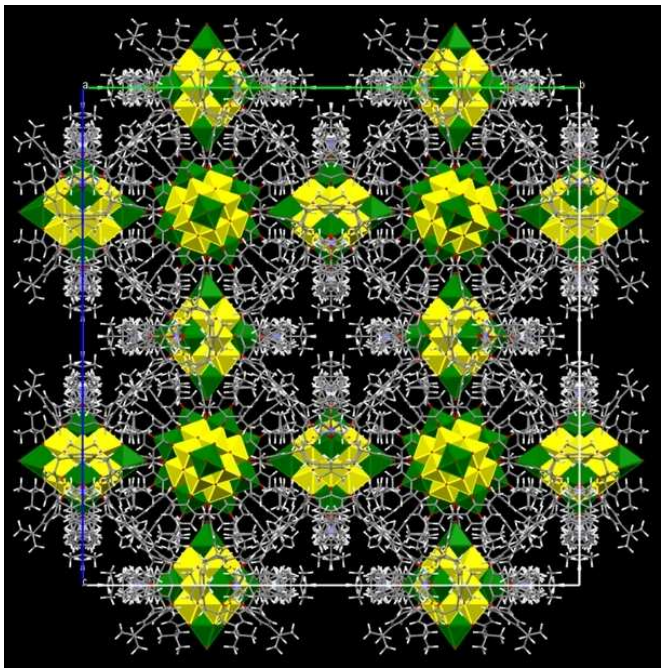

Figure 4. Packing diagram for **1** viewed down the *a*-axis of the cell highlighting the octahedral arrangement of clusters. The metal ions are in polyhedral format, the rest of the atoms in ball and stick. Fe(octahedron) = green, Fe(cuboctahedron) = yellow, O = red, C = grey, H = white.

Tb, Dy).[15,16] The metal-oxygen core of **1** is similar to the "Super Lindqvist" complex $[HFe^{III}_{19}O_{14}(OEt)_3]$ (synthesised solvothermally) which has an additional Fe ion at its centre.[17] There are just two other stellated cuboctahedra reported: the first is a supramolecular $[Pd_{18}L_{24}]$ cage constructed with a polypyridine ligand,[18] and the second a $[Mn^{III}_{18}]$ 'superoctahedron' built with an aminoalcohol.[19]

Magnetic susceptibility (χ) and magnetisation (M) data were measured on a polycrystalline sample of **1** in the T = 300–2 K, B = 0.1 T and T = 0.4–10 K, B = 0.5–32.5 T temperature and field ranges, respectively. These data are plotted as the χT product versus T in Figure 5 and as M vs B in Figures 5 and S7. At 300 K the value of χT (42.6 $cm^3 K mol^{-1}$) is well below that expected for eighteen non-interacting $S = 5/2$ ions (78.75 $cm^3 K mol^{-1}$), assuming $g_{Fe} = 2.00$. As the temperature is lowered the value of χT decreases rapidly to a value of 9.2 cm^3 K mol^{-1} at $T = 2.0$ K. The magnetisation data at $T = 0.4$ K rise rapidly up to $B = 1$–2 T (~4 μ_B), then increase in a more linear like fashion up to $B = 12$ T (~15 μ_B), above which the magnetisation rises more slowly reaching a plateau of sorts (~17.5 μ_B) at $B = 32.5$ T. This behaviour is indicative of strong, competing antiferromagnetic exchange interactions, with the sharp initial rise of the magnetisation likely ascribed to a canted moment.

The magnetic susceptibility and magnetisation data could in principle be simulated using an isotropic spin-

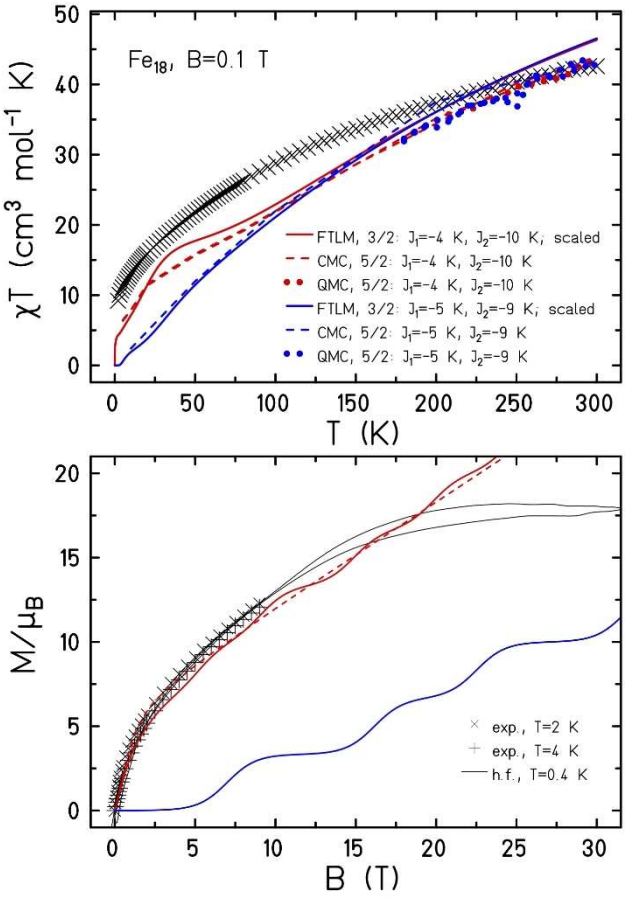

Figure 5. Plot of χT versus T (top) and M vs B (bottom) for **1**. The curves coloured in red represent the best simulations of the experimental (x) data. Thin black curves for M vs B show high-field magnetisation data collected up to 32.5 T. The blue simulation curves show a nearby parameterisation for comparison. See main text for details.

Hamiltonian $\widehat{H} = -2 \sum_{i<j} J_{ij} \widehat{\vec{s}}_i \cdot \widehat{\vec{s}}_j$. However, due to the large dimension (101,559,956,668,416) of the related Hilbert space an exact[20] or approximate[21] diagonalisation of the Hamiltonian and a subsequent calculation of observables is virtually impossible. We thus resort to more drastic approximations to obtain order of magnitude estimates for the exchange interactions. A reasonable reduction of parameters is given by assuming just two exchange interactions, J_1 along the edges of the cuboctahedron and J_2 along the edges of the square pyramids to the respective caps (Figure S6). As Figure 5 shows, large scale classical Monte-Carlo calculations agree well with scaled-up finite-temperature Lanczos calculations[21] performed with fictitious spins $S = 3/2$ for $J_1 = -4$ K, $J_2 = -10$ K and $g_{Fe} = 2.0$ (red curves). The magnetisation is particularly well met up to 10 T. One should, however, keep in mind that both approximations are rough, and that the assumption of just two exchange parameters oversimplifies the situation. The plateau-like flattening of M vs B is thus not modelled. Nevertheless, the result shows that antiferromagnetic exchange interactions characterise the cluster. It is strongly frustrated and situated in a parameter space close to scenarios with gapped singlet ground states that behave very differently, as demonstrated by the blue curves (in particular M vs B).

Heat capacity (c_p) data, measured on a polycrystalline sample of **1** in the $T = 20$–0.4 K range and $B = 0$, 1, 3 and 9 T, yield a rather straight temperature dependence in a log-log plot (Figure S8). The theory approximation cannot reproduce $c_p(T,B)$ since it would require an accurate account of the low-lying energy levels. At temperatures as low as 0.4 K, the entropy (S, inset of Figure S8, derived from c_p), which is fully suppressed in external fields, reaches *ca.* 0.5 R for $B = 0$ T. The presence of a low-temperature zero-field entropy agrees with the observation that a gapped model (blue curves in Figure 5) does not reproduce the magnetization. Further insight can be obtained from evaluating the magnetocaloric effect (MCE), specifically, the temperature dependences of the magnetic entropy change, $-\Delta S_m$, and adiabatic temperature change, ΔT_{ad}, for applied field changes $\Delta B = 1$, 3 and 9 T (Figure 6). These data are calculated from $c_p(T,B)$ as well as $M(T,B)$ in case of $-\Delta S_m$ (Figure S7), following standard procedures.[8] Overall, the MCE is modest with maximum values of $-\Delta S_m = 1.4$, $R = 2.7$ Jkg^{-1}K^{-1} and $\Delta T_{ad} = 1.5$ K for $\Delta B = 9$ T. An interesting and rather unusual observation is that an *inverse* MCE develops above *ca.* 10 K, resulting in $-\Delta S_m = -0.5$, $R = -1.0$ Jkg^{-1}K^{-1} and $\Delta T_{ad} = -0.15$ K, both at 20 K, for any ΔB lower than 3 T. The inverse MCE is a clear signature of relatively strong antiferromagnetic correlations.[22,23] The observation of either inverse MCE or conventional, though weaker, paramagnetic-like magnetocaloric response is the result of a delicate balance between the temperature and strengths of the antiferromagnetic correlations and applied field, which tend to cancel mutually. Indeed, higher fields promote a larger decoupling between the spin centres, resulting in a crossover from inverse to direct MCE, as experimentally observed after increasing ΔB from 3 to 9 T. At low fields, the inverse-direct MCE crossover takes place as the temperature decreases below ~10 K (Figure 6). This behaviour can be well accounted for by the onset of the canted moment observed in the magnetisation measurements. In conclusion, **1** turns out to be a highly frustrated antiferromagnetic cluster with elevated low-temperature zero-field entropy possibly stemming from competing and varying interactions beyond a J_1–J_2 model.

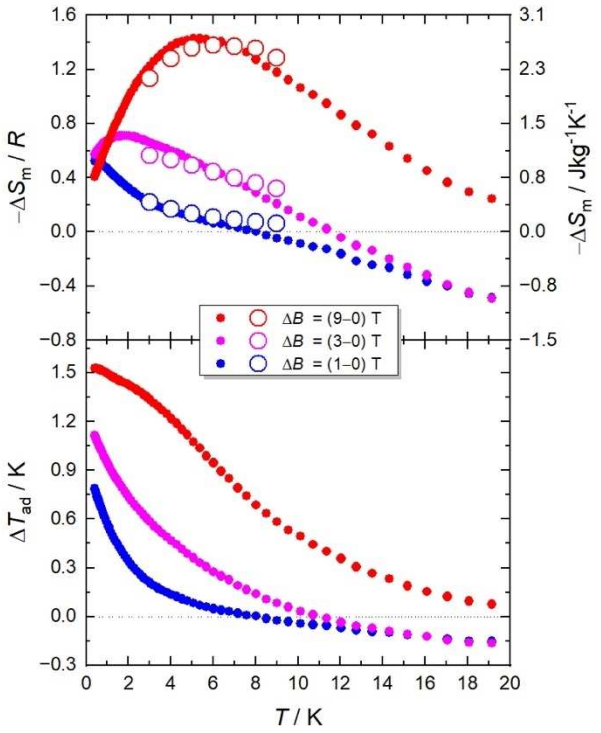

Figure 6. Plot of $-\Delta S_m$ (top) and ΔT_{ad} (bottom) versus T for **1**, for applied field changes ΔB, as labelled. The $-\Delta S_m$ data are normalised by the gas constant R (left axis) and expressed in Jkg^{-1}K^{-1} (right axis). Small, filled symbols are obtained from the heat capacity data (Figure S8), whereas large, open circles represent the outcome of the respective Maxwell relation applied to the magnetization data (Figure S7).

Acknowledgements

EKB, ABC thank The Leverhulme Trust (RPG-2021-176). DJL, HN thank the JSPS (grant no. PE22724). ME thanks the Spanish MICINN (grant no. PID2021-124734OB- C21).

Conflict of Interest

The authors declare no conflict of interest.

Data Availability Statement

The data that support the findings of this study are available from the corresponding author upon reasonable request.

Keywords: Fe^{III} · calix[4]arene · stellated cuboctahedron · spin frustration · magnetic measurements

[1] G. Toulouse, *Comm. Phys.* **1977**, *2*, 115–119.
[2] S. Kirkpatrick, *Phys. Rev. B* **1977**, *16*, 4630–4641.
[3] See for example, a) A. P. Ramirez, *Annu. Rev. Mater. Sci.* **1994**, *24*, 453; b) J. Greedan, *J. Mater. Chem.* **2001**, *11*, 37; c) R. Moessner, *Can. J. Phys.* **2001**, *79*, 1283; d) S. T. Bramwell, M. J. P. Gingras, *Science* **2001**, *294*, 1495–1501.
[4] O. Kahn, *Chem. Phys. Lett.* **1997**, *265*, 109–114.
[5] J. K. McCusker, E. A. Schmitt, D. N. Hendrickson, *High Spin Inorganic Clusters: Spin Frustration in Polynuclear Manganese and Iron Complexes.* In: D. Gatteschi, O. Kahn, J. S. Miller, F. Palacio, (eds) Magnetic Molecular Materials. NATO ASI Series, vol 198. Springer, Dordrecht **1991**.
[6] J. Schnack, *Dalton Trans.* **2010**, *39*, 4677–4686.
[7] M. L. Baker, G. A. Timco, S. Piligkos, J. S. Mathieson, H. Mutka, F. Tuna, P. Kozłowski, M. Antkowiak, T. Guidi, T. Gupta, H. Rath, R. J. Woolfson, G. Kamieniarz, R. G. Pritchard, H. Weihe, L. Cronin, G. Rajaraman, D. Collison, E. J. L. McInnes, R. E. P. Winpenny, *PNAS* **2012**, *109*, 19113–19118.
[8] M. Evangelisti, E. K. Brechin, *Dalton Trans.* **2010**, *39*, 4672–4676.
[9] N. Hoshino, M. Nakano, H. Nojiri, W. Wernsdorfer, H. Oshio, *J. Am. Chem. Soc.* **2009**, *131*, 5100–15101.
[10] O. Cador, D. Gatteschi, R. Sessoli, F. K. Larsen, J. Overgaard, A.-L. Barra, S. J. Teat, G. A. Timco, R. E. P. Winpenny, *Angew. Chem.* **2004**, *116*, 5308–5312; *Angew. Chem. Int. Ed.* **2004**, *43*, 5196–5200.
[11] R. J. Woolfson, G. A. Timco, A. Chiesa, I. J. Vitorica-Yrezabal, F. Tuna, T. Guidi, E. Pavarini, P. Santini, S. Carretta, R. E. P. Winpenny, *Angew. Chem.* **2016**, *128*, 9002–9005; *Angew. Chem. Int. Ed.* **2016**, *55*, 8856–8859.
[12] V. O. Garlea, S. E. Nagler, J. L. Zarestky, C Stassis, D. Vaknin, P. Kögerler, D. F. McMorrow, C. Niedermayer, D. A. Tennant, B. Lake, Y. Qiu, M. Exler, J. Schnack, M. Luban, *Phys. Rev. B* **2006**, *73*, 024414.
[13] a) B. Cage, F. A. Cotton, N. S. Dalal, E. A. Hillard, B. Rakvin, C. M. Ramsey, *J. Am. Chem. Soc.* **2003**, *125*, 5270–5271; b) D. Dai, M.-H. Whangbo, *J. Chem. Phys.* **2004**, *121*, 672–680.
[14] C. D. Gutsche, in *Calixarenes: An Introduction*, The Royal Society of Chemistry, Cambridge, 2nd edn, **2008**, ch. 2. pp. 27–160.
[15] a) L. R. B. Wilson, M. Coletta, M. Evangelisti, S. Piligkos, S. J. Dalgarno, E. K. Brechin, *Dalton Trans.* **2022**, *51*, 4213–4226; b) S. Sanz, K. Ferreira, R. D. McIntosh, S. J. Dalgarno, E. K. Brechin, *Chem. Commun.* **2011**, *47*, 9042–9044; c) M. Coletta, R. McLellan, S. Sanz, K. J. Gagnon, S. J. Teat, E. K. Brechin, S. J. Dalgarno, *Chem. Eur. J.* **2017**, *23*, 14073–14079.
[16] a) A. Arbaoui, C. Redshaw, M. R. J. Elsegood, V. E. Wright, A. Yoshizawa, T. Yamato, *Chem. Asian J.* **2010**, *5*, 621–633; b) M. Coletta, R. McLellan, P. Murphy, B. T. Leube, S. Sanz, R. Clowes, K. J. Gagnon, S. J. Teat, A. I. Cooper, M. J. Paterson, E. K. Brechin, S. J. Dalgarno, *Chem. Eur. J.* **2016**, *22*, 8791–8795.
[17] O. Nachtigall, M. Kusserow, R. Clérac, W. Wernsdorfer, M. Menzel, F. Renz, J. Mrozinski, J. Spandl, *Angew. Chem.* **2015**, *127*, 10503–10506; *Angew. Chem. Int. Ed.* **2015**, *54*, 10361–10364.
[18] Q.-F. Sun, S. Sato, M. Fujita, *Nat. Chem.* **2012**, *4*, 330–333.
[19] A.-J. Zhou, J.-D. Leng, J.-S. Hua, M.-L. Tong, *Dalton Trans.* **2013**, *42*, 9428–9431.
[20] a) R. Schnalle, J. Schnack, *Int. Rev. Phys. Chem.* **2010**, *29*, 403–452.
[21] a) J. Jaklic, P. Prelovšek, *Phys. Rev. B* **1994**, *49*, 5065; b) J. Schnack, J. Richter, R. Steinigeweg, *Phys. Rev. Research* **2020**, *2*, 013186; c) N. A. G. Bandeira, O. Sadeghi, T. J. Woods, Y.-Z. Zhang, J. Schnack, K. R. Dunbar, M. Nyman, C. Bo, *J. Phys. Chem. A* **2017**, *121*, 1310.
[22] P. J. von Ranke, N. A. de Oliveira, B. P. Alho, E. J. R. Plaza, V. S. R. de Sousa, L. Caron, M. S. Reis, *J. Phys. Condens. Matter* **2009**, *21*, 056004.
[23] J. W. Sharples, D. Collison, E. J. L. McInnes, J. Schnack, E. Palacios, M. Evangelisti, *Nat. Commun.* **2014**, *5*, 5321.

Manuscript received: March 25, 2024
Accepted manuscript online: June 17, 2024
Version of record online: ■■, ■■

Zuschrift

Spin Frustration

L. R. B. Wilson, A. B. Canaj, D. J. Cutler, L. J. McCormick McPherson, S. J. Coles, H. Nojiri,* M. Evangelisti,* J. Schnack,* S. J. Dalgarno,* E. K. Brechin* _____ **e202405666**

Stellated cuboctahedron of Fe^{III}

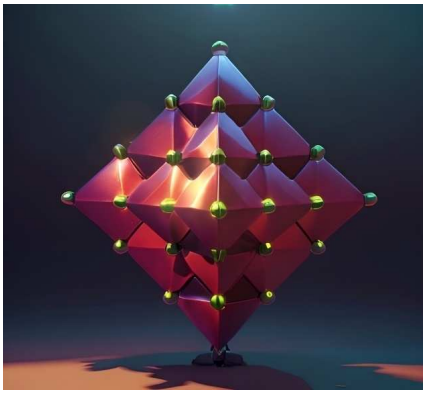

A stellated cuboctahedron of Fe^{III} ions can be constructed using *p*-tert-butylcalix[4]arene (H_4TBC[4]) under solvothermal reaction conditions. The topological arrangement of the metal ions leads to significant spin frustration arising from the high symmetry. A crossover between inverse and direct magnetocaloric effects is observed at 10 K for applied-field changes lower than 3 T.